Available online at www.sciencedirect.com
ScienceDirect
Ceramics International 37 (2011) 825–833
CERAMICS INTERNATIONAL
www.elsevier.com/locate/ceramint

Characteristics of exothermic reaction fronts in the gasless combustion system

Tae Sung Kang [a], Chang-Ho Park [b], Sang Hwan Kim [a,*]

[a] Department of Chemical Engineering, Konkuk University, Seoul 143-701, Republic of Korea
[b] Department of Chemical Engineering, Kyunghee University, Yongin 449-701, Republic of Korea

Received 13 April 2010; received in revised form 20 August 2010; accepted 12 October 2010
Available online 17 November 2010

Abstract

Gasless combustion model of the self-propagating high-temperature synthesis process was numerically studied in the non-adiabatic cylindrical sample. The model equations, which are very stiff in the dimension of length as well as time, were solved using finite difference method on adaptive meshes. Travelling waves with constant pattern were observed for adiabatic systems. For higher values of heat of reaction and activation energy, combustion fronts started to oscillate for adiabatic and non-adiabatic systems. Simple and complex oscillatory fronts were observed. Multi-peak and irregular oscillations were also detected to presumably result in the gasless chaotic combustion. In oscillatory fronts the temperature can overshoot the adiabatic reaction temperature to result in the complete conversion of solid reactant. In the two dimensional non-adiabatic cylindrical sample in the domain of longitudinal and angular directions, oscillatory piston waves were observed. In addition asymmetrical fingering as well as rotating waves were detected for an asymmetrical perturbation. For the adiabatic annulus cylindrical sample, the velocity of propagating fronts increased with time and the temperature overshooted the adiabatic reaction temperature if the sample were ignited from the inside. If the sample were ignited from the outside, the velocity of propagating fronts decreased with time and the temperature again overshooted the adiabatic reaction temperature. For smaller diameter of sample, the temperature increased very slowly with time for inside ignition. The temperature after ignition increased very fast overshooting the adiabatic reaction temperature for outside ignition. After several oscillations, the reaction rate decreased and the region with very slow reaction was established.

Keywords: Solid state reaction; Refractory; Cutting tools

1. Introduction

Self-propagating high-temperature synthesis is potentially an energy-efficient process to produce refractory ceramics, ceramic composites, and intermetallics. Conventional method for producing refractory ceramic material involves heating the solid metal in the furnace for several hours at high temperatures. Furthermore, the product quality is often affected adversely by incomplete conversion of solid reactant. However, thermal effects generated due to the extreme heat of reaction and high activation energy of the synthesis reaction can be utilized to run the reaction in the self-sustaining regime. Once ignited, the sharp combustion front is formed and propagates through the reactants in the form of combustion wave. As the combustion wave advances, the reactant is converted to the product. The advantages of self-propagating high-temperature synthesis process include very low energy consumption, short synthesis time, and high purity of the product. In the production of refractory ceramic material, the synthesis and densification steps may be combined into one operation. Since the reaction takes place in the combustion regime rather than the kinetic regime, it is difficult to control and predict the processes. The efficient way to understand these systems is to gain the insight into the dynamics of such systems. Since there are a large number of system parameters which govern the behavior of the systems, experiments alone cannot be used to understand these systems. Numerical modeling provides an important alternative to study these systems and to understand the mass and heat transfer characteristics of the systems.

Maksimov et al. [1] used the term ''gasless composition'' to the systems which burn without the starting, intermediate or

* Corresponding author. Tel.: +82 2 450 3507; fax: +82 2 458 3504.
E-mail address: sanghkim@konkuk.ac.kr (S.H. Kim).

0272-8842/$36.00
doi:10.1016/j.ceramint.2010.10.017

Nomenclature

Bi	Biot number, hR/λ
c_S	concentration of the solid S (kg m^{-3})
C_s	dimensionless concentration of the solid S, $\frac{c_S}{c_{si}}$
$\overline{C_p}$	Heat capacity of solid S and gas (or solid) M (J kg^{-1} K^{-1})
$\overline{\rho C_p}$	$\rho_{M0}c_{PM}\varepsilon + \rho_{S0}c_{PS}(1-\varepsilon)$
E	activation energy (J mol^{-1})
h	heat transfer coefficient (J m^{-1} K^{-1})
ΔH	heat of reaction (J kg^{-1})
k_0	pre-exponential factor (s^{-1})
r	radial length (m)
R	radius of the sample (m)
R_g	gas constant
t	time (s)
t^*	scaling time, $(\overline{\rho C_p}R_gT_*^2\exp(E/R_gT_*))/(Ek_0(-\Delta H)c_{si})$
T	temperature (K)
T_*	reference temperature (=adiabatic reaction temperature) (K)
z	axial length (m)
z^*	scaling axial length, $1/\sqrt{\overline{\rho C}/\lambda t*}$
Z	dimensionless axial length, $z\sqrt{\overline{\rho C_p}/\lambda t*}$

Greek symbols

α	dimensionless heat transfer coefficient, $2ht^*/\overline{\rho C_p}R$
β	dimensionless activation energy, R_gT*/E
γ	dimensionless heat of reaction $(\overline{\rho C_p}R_gT_*^2)/C_{si}E(-\Delta H)$
ε	porosity of solid S and gas (or solid) M
Δ	stability parameter
θ	angular coordinate (^{o})
Θ	dimensionless temperature $(E/(R_gT_*))((T-T_*)/T_*)$
λ	thermal conductivity (J m^{-1} K$^{-1)}$
ξ	dimensionless radial length (r/R)
ρ	density (kg m^{-3})
$\overline{\rho}$	density of solid S and gas (or solid) M (Kg m^{-3})
τ	dimensionless time, t/t^*
ϕ	dimensionless angular coordinate, $\theta/2\pi$

Superscripts

*	scaling factor

Subscripts

a	ambient condition
i	initial condition
o	boundary condition

final materials forming the gas phase. Convenient models of such a gasless composition appeared to be thermites, which burn without the formation of gaseous reaction products. Unfortunately most of thermites described previously were unsuitable because the burning rate displayed a marked dependence on the pressure. This is apparently linked with the formation of gas at combustion temperatures. Therefore an attempt was made to obtain the gasless system by decreasing the combustion temperature by diluting the starting materials with end products, so as not to complicate the physicochemical nature of the processes associated with the combustion. They selected an iron–aluminum thermite since the physicochemical properties of the starting materials and final products of this thermite had been studied in detail.

Shkadinskii et al. [2] studied the instability region of parameters where steady-state combustion was unstable in the adiabatic gasless systems. They proposed the criterion Δ to differentiate stable combustion from unstable one. If $\Delta \geq 1$, the stable combustion takes place. But if $\Delta < 1$, then the combustion proceeds in the unstable regime. The decrease of combustion temperature, the increase of the inert component in the starting materials or the dilution of starting materials with end products may change the stable combustion to unstable ones.

The gasless combustion has been studied both theoretically and experimentally by Maksimov et al. [1], Shkadinskii et al. [2], Merzhanov and Borovinskaya [3], and Dimitriou et al. [4]. Recently Ivleva and Merzhanov [5–8] predicted the solid flame chaos in the three dimensional model considering the heat conduction in the longitudinal, radial and angular directions. For the majority of gasless combustion systems, many people tried to eliminate or at least to suppress the instability effects because they impair the reaction control and lead to the non-uniform product and the incomplete conversion of the reactant.

The purpose of this study is to numerically analyze the gasless combustion model of self-propagating high-temperature synthesis process in the non-adiabatic cylindrical samples considering the longitudinal and angular heat conduction. Simulating the gasless combustion in two dimensional directions, gives us to understand the stability of exothermic reaction fronts and the behavior of travelling, oscillating, fingering, rotating and erratic waves during its process under the wide range of operating conditions. The insight gained from this study helps us to understand the behavior of the self-propagating high-temperature synthesis process, which is a necessary prerequisite to our ability to effectively control the process.

2. Model formulation

The cylindrical sample with the uniform distribution of solid reactant is studied in the gasless non-adiabatic combustion system. The reaction is ignited by a short-term energy source such as the resistively heated tungsten wire or graphite. Once ignited, the reaction continues on its own in the form of a steep combustion front which separates unreacted solid from the product. The reaction between the solid S and the reacting gas (or the secondary solid) M resulting in the gasless solid product P, occurs in the following manner.

$$S(s) + M(g \text{ or } s) \rightarrow P(s) \quad (1)$$

Modeling of gasless combustion process involves the mass and energy transport and their generation or consumption. In

order to make the model solvable by current techniques of numerical analysis, several simplification assumptions are made as follows:

(1) The heterogeneous system consisting of solid particles and reacting gas or mixture of two different solid particles may be treated as though it were homogeneous and a hypothetical continuum considered.
(2) A heterogeneous reaction occurs between the solid S and the gas M or the solid S and secondary solid M. The reaction rate may be represented by the following equation:

$$-r_s = k\,C_S^n C_M^m \tag{2}$$

The reaction rate was simplified to be the first order with respect to the solid S and independent on the gas (or the solid) M (i.e., $n = 1$, $m = 0$).
(3) The physical properties such as density, heat capacity, thermal conductivity and diffusion coefficients, are assumed to be constant.
(4) The melting effects and heat of fusion in the system are not considered.

The governing equations describing the gasless combustion in the cylindrical sample are written in the following way:

Energy balance:

$$\overline{\rho C_p}\frac{\partial T}{\partial t} = \lambda\left(\frac{\partial^2 T}{\partial z^2} + \frac{\partial^2 T}{\partial r^2} + \frac{1}{r}\frac{\partial T}{\partial r} + \frac{1}{r^2}\frac{\partial^2 T}{\partial \theta^2}\right) + k_0 \exp\left(-\frac{E}{R_g T}\right)(-\Delta H)C_S \tag{3}$$

Mass balance:

$$(1-\varepsilon)\frac{\partial c_S}{\partial t} = -k_0 \exp\left(-\frac{E}{R_g T}\right)C_S \tag{4}$$

Initial and boundary conditions can be written as follows:

$$t = 0, \quad 0 \le Z < \infty, \quad 0 \le \theta \le 2\pi, \quad 0 \le r \le R: \quad T = T_i, \quad c_S = c_{S_i} \tag{5}$$

$$z = 0, \quad t > 0, \quad 0 \le \theta \le 2\pi, \quad 0 \le r \le R: \quad T = T_0, \quad c_S = c_{S_i} \tag{6}$$

$$z = \infty, \quad t > 0, \quad 0 \le \theta \le 2\pi, \quad 0 \le r \le R: \quad T = T_i, \quad c_S = c_{S_i} \tag{7}$$

$$r = R, \quad t > 0, \quad 0 \le \theta \le 2\pi, \quad 0 < z < \infty: \quad -\lambda\frac{\partial T}{\partial r} = h(T - T_a), \quad \frac{\partial c_s}{\partial r} = 0 \tag{8}$$

Here T is the temperature; c_S is the concentration of the solid S; ΔH is the heat of reaction; ρ and C_p are the density and heat capacity; λ is the thermal conductivity of the sample; k_0 is the pre-exponential factor; E is the activation energy; R_g is the gas constant; h is the heat transfer coefficient between the sample and the surroundings; T_i is the initial temperature of the sample; T_o is the temperature of the igniter wall; ε is the porosity of the sample for the gas–solid system or the volume fraction of the solid in the sample for the solid–solid system. The term $\overline{\rho C_p}$ represents the contribution of heat capacity of the solid particles and the gas or the mixture of two different solid particles. The whole variables and parameters appearing in this paper are described in the nomenclature. To render the equations dimensionless, the following scaling relations are used for the independent and dependent variables in the following way:

$$\tau = \frac{t}{t*}, \quad t* = \frac{\overline{\rho C_p} R_g T_*^2 \exp(E/R_g T_*)}{E k_0 (-\Delta H) c_{Si}}$$

$$Z = \frac{z}{z*} = z\sqrt{\frac{\rho C_p}{\lambda t*}}, \quad z* = \frac{1}{\sqrt{\rho C_p/\lambda t*}}, \quad \phi = \frac{\theta}{2\pi}, \quad \xi = \frac{r}{R} \tag{9}$$

$$c_s = \frac{c_S}{c_{Si}}, \quad \Theta = \frac{E}{R_g T_*}\frac{T - T_*}{T_*}, \quad \gamma = \frac{\overline{\rho C_p} R_g T_*^2}{c_{Si} E(-\Delta H)}$$

$$\beta = \frac{R_g T_*}{E}, \quad Bi = \frac{hR}{\lambda}, \quad \alpha = \frac{2ht_*}{\overline{\rho C_p} R}, \quad \delta = \frac{\lambda t_*}{4\overline{\rho C_p}\pi^2 R^2}$$

The parameters γ and β are defined as the dimensionless heat of reaction and activation energy, respectively. Low γ and β values represent the system with high heat of reaction and high activation energy and vice versa. The system temperature is made dimensionless using the characteristic temperature T_* (in our case, the adiabatic reaction temperature). Thus, the dimensionless temperature values Θ are typically negative when the temperature of the system is lower than the characteristic temperature T_*. The parameter α describes the dimensionless heat transfer coefficient between the system and the surroundings. Therefore $\alpha = 0$ implies the adiabatic operation of combustion system while $\alpha \neq 0$ denotes the non-adiabatic combustion system.

Substituting into the dimensional equations results in the following dimensionless equations:

$$\frac{\partial \Theta}{\partial \tau} = \frac{\partial^2 \Theta}{\partial Z^2} + \delta\left\{4\pi^2\left(\left(\frac{1}{\xi}\right)\left(\frac{\partial \Theta}{\partial \xi}\right) + \left(\frac{\partial^2 \Theta}{\partial \xi^2}\right)\right) + \left(\frac{1}{\xi^2}\right)\left(\frac{\partial^2 \Theta}{\partial \phi^2}\right)\right\} + C_S \exp\left(\frac{\Theta}{1 + \beta\Theta}\right) \tag{10}$$

$$(1-\varepsilon)\frac{\partial C_s}{\partial \tau} = -\gamma C_s \exp\left(\frac{\Theta}{1 + \beta\Theta}\right) \tag{11}$$

Initial and boundary conditions are:

$$\tau = 0, \quad 0 \le Z < \infty, \quad 0 \le \phi \le 1 \quad 0 \le \xi \le 1: \quad \Theta = \Theta_i, \quad C_s = 1 \tag{12}$$

$$Z = 0, \quad \tau > 0, \quad 0 \le \phi \le 1, \quad 0 \le \xi \le 1: \quad \Theta = \Theta_0, \quad C_s = 1 \tag{13}$$

$$Z=\infty,\quad \tau>0,\quad 0\le\phi\le 1,\quad 0\le\xi\le 1:\quad \Theta=\Theta_i,\quad C_s=1 \tag{14}$$

$$\xi=1,\quad \tau>0,\quad 0\le\phi\le 1,\quad 0<Z<\infty:\quad \frac{\partial\Theta}{\partial\xi}=Bi(\Theta-\Theta_{\mathrm{i}}),\frac{\partial C_{\mathrm{s}}}{\partial\xi}=0 \tag{15}$$

2.1. One-dimensional model

We assume that the system is angularly symmetrical and the importance of radial gradients is marginal. Then, Eqs. (10)–(15) reduce to the simplified one-dimensional model in the following way.

$$\frac{\partial\Theta}{\partial\tau}=\frac{\partial^2\Theta}{\partial Z^2}+C_{\mathrm{S}}\exp\left(\frac{\Theta}{1+\beta\Theta}\right)-\alpha(\Theta-\Theta_i) \tag{16}$$

$$(1-\varepsilon)\frac{\partial C_{\mathrm{s}}}{\partial\tau}=-\gamma C_{\mathrm{S}}\quad\exp\left(\frac{\Theta}{1+\beta\Theta}\right) \tag{17}$$

Initial and boundary conditions are represented as follows:

$$\tau=0,\quad 0\le Z<\infty,\quad 0\le\phi\le 1,\quad 0\le\xi\le 1:\quad \Theta=\Theta_i,\quad C_s=1 \tag{18}$$

$$Z=0,\quad \tau>0,\quad 0\le\phi\le 1,\quad 0\le\xi\le 1:\quad \Theta=\Theta_0 \tag{19}$$

$$Z=\infty,\quad \tau>0,\quad 0\le\phi\le 1,\quad 0\le\xi\le 1:\quad \Theta=\Theta_i \tag{20}$$

2.2. Two-dimensional model

The system is strongly nonlinear, so that the occurrence of angular temperature gradients cannot be neglected. But the importance of radial gradients is marginal and temperature distribution on the surface of the cylindrical sample ($\xi = 1$) is considered. For this condition Eqs. (10)–(15) reduce to Eqs. (21)–(26) as follows:

$$\frac{\partial\Theta}{\partial\tau}=\frac{\partial^2\Theta}{\partial Z^2}+\delta\frac{\partial^2\Theta}{\partial\phi^2}+C_{\mathrm{S}}\quad\exp\left(\frac{\Theta}{1+\beta\Theta}\right)-\alpha(\Theta-\Theta_i) \tag{21}$$

$$(1-\varepsilon)\frac{\partial C_{\mathrm{S}}}{\partial\tau}=-\gamma C_{\mathrm{S}}\exp\left(\frac{\Theta}{1+\beta\Theta}\right) \tag{22}$$

Initial and boundary conditions are:

$$\tau=0,\quad 0\le Z<\infty,\quad 0\le\phi\le 1,\quad 0\le\xi\le 1:\quad \Theta=\Theta_i,\quad C_{\mathrm{S}}=1 \tag{23}$$

$$Z=0,\quad \tau>0,\quad 0\le\phi\le 1,\quad 0\le\xi\le 1:\quad \Theta=\Theta_0 \tag{24}$$

$$Z=\infty,\quad \tau>0,\quad 0\le\phi\le 1,\quad 0\le\xi\le 1:\quad \Theta=\Theta_i \tag{25}$$

$$\phi=\phi\,\text{and}\,\phi=\phi+1,\tau>0,\quad 0<Z<\infty,\quad 0\le\xi\le 1:\quad \Theta(\phi)=\Theta(\phi+1),\quad C_{\mathrm{S}}(\phi)=C_{\mathrm{S}}(\phi+1) \tag{26}$$

Eq. (26) is subject to so called periodic boundary conditions. Periodic boundary conditions result from the assumptions that the accessible structure is near the surface and represents a thin annular space which can be unfolded.

3. Results from numerical simulation

The set of equations describing the gasless combustion are highly coupled and nonlinear partial differential equations. They exhibit steep spatial gradients in the temperature and

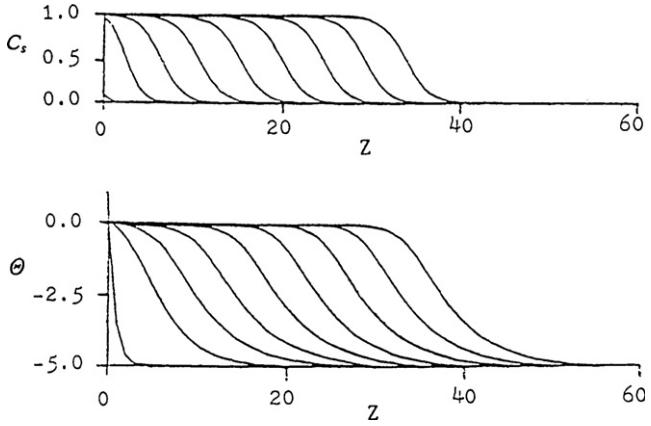

Fig. 1. Constant pattern profile front in one-dimensional adiabatic system. $\alpha = 0.0$, $\beta = 0.1$, $\gamma = 0.2$, $\Theta_{\mathrm{i}} = -5.0$, $\Theta_{\mathrm{o}} = 0.0$, $\varepsilon = 0.5$, $\Delta = 1.57$. From the left profile line, τ is (1) 0.1, (2) 21, (3) 45, (4) 60, (5) 93, (6) 117, (7) 141, (8) 165 and (9) 189, respectively.

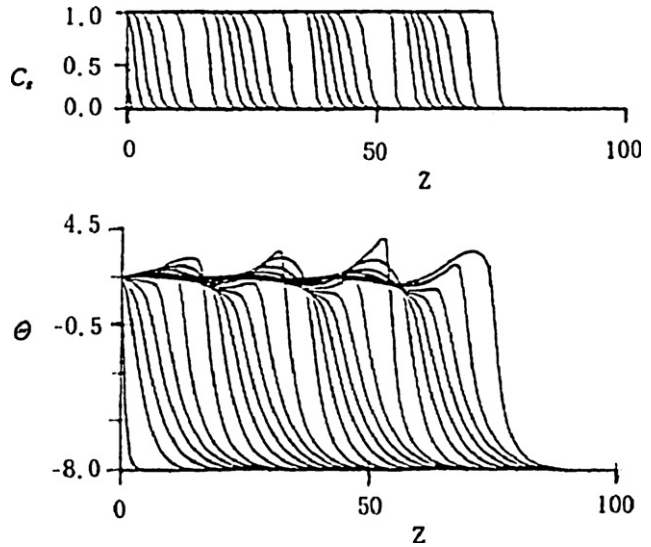

Fig. 2. Oscillatory front in one-dimensional adiabatic system. $\alpha = 0.0$, $\beta = 0.03$, $\gamma = 0.1$, $\Theta_{\mathrm{i}} = -8.0$, $\Theta_{\mathrm{o}} = 2.0$, $\varepsilon = 0.5$, $\Delta = 0.835$.

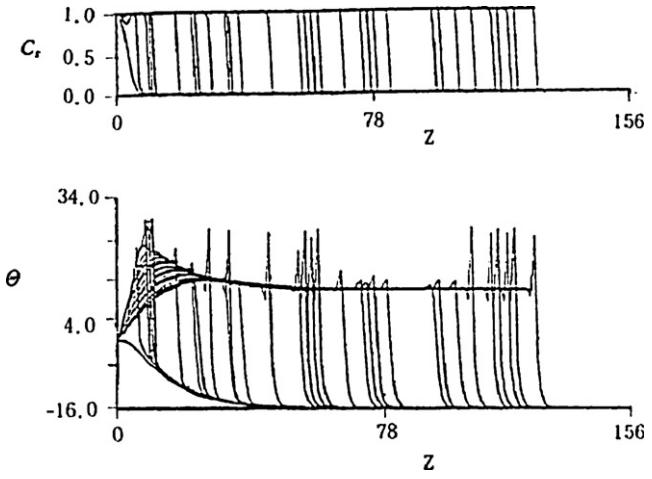

Fig. 3. Multipeak oscillatory front in one-dimensional adiabatic system. $\alpha = 0.0$, $\beta = 0.03$, $\gamma = 0.03$, $\Theta_i = -16.0$, $\Theta_o = 0.0$, $\varepsilon = 0.5$, $\Delta = 0.798$.

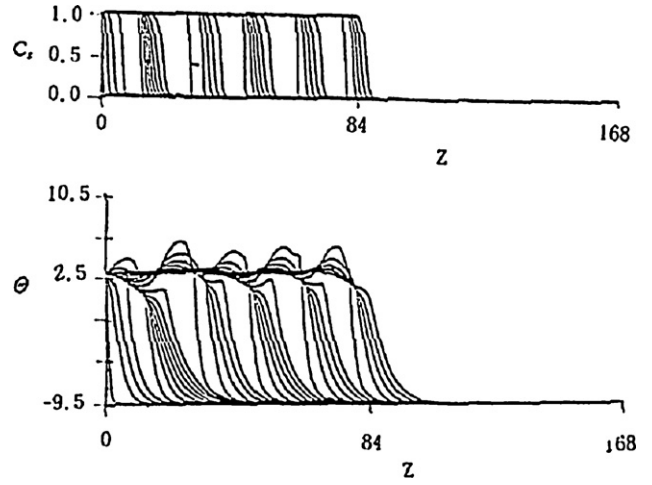

Fig. 4. Oscillatory front in one-dimensional adiabatic system. $\alpha = 0.0$, $\beta = 0.03$, $\gamma = 0.0$, $\Theta_i = -9.5$, $\Theta_o = 3.0$, $\varepsilon = 0.5$, $\Delta = -0.075$.

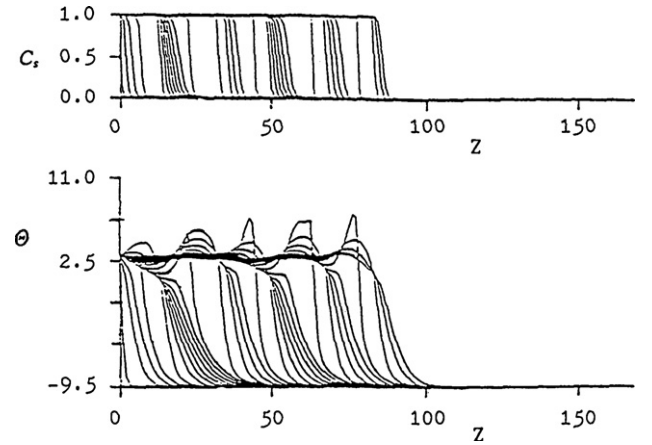

Fig. 5. Oscillatory front in one-dimensional non-adiabatic system. $\alpha = 0.0001$, $\beta = 0.03$, $\gamma = 0.03$, $\Theta_i = -9.5$, $\Theta_o = 3.0$, $\varepsilon = 0.5$, $\Delta = 0.198$.

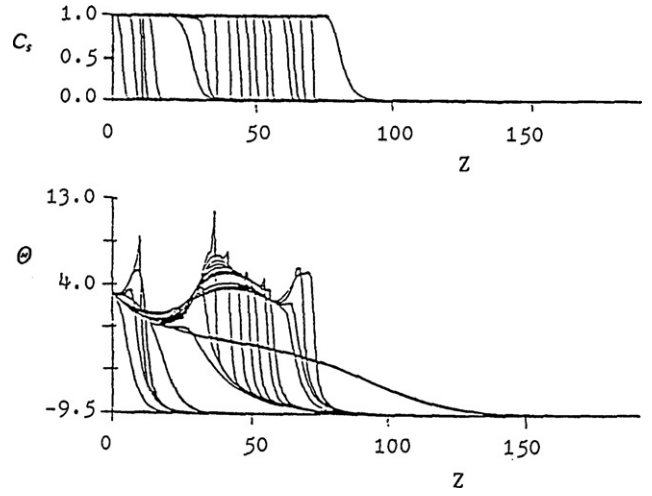

Fig. 6. Complex oscillatory front in one-dimensional non-adiabatic system. $\alpha = 0.001$, $\beta = 0.03$, $\gamma = 0.03$, $\Theta_i = -9.5$, $\Theta_o = 3.0$, $\varepsilon = 0.5$, $\Delta = 0.198$.

concentration domain. An intricate formulation involving finite difference approximation on two-dimensional adaptive grids is used. Details of the adaptive mesh algorithm are available in the literature of Park [9].

Travelling wave of constant pattern profiles with constant velocity propagates through the adiabatic system as shown in

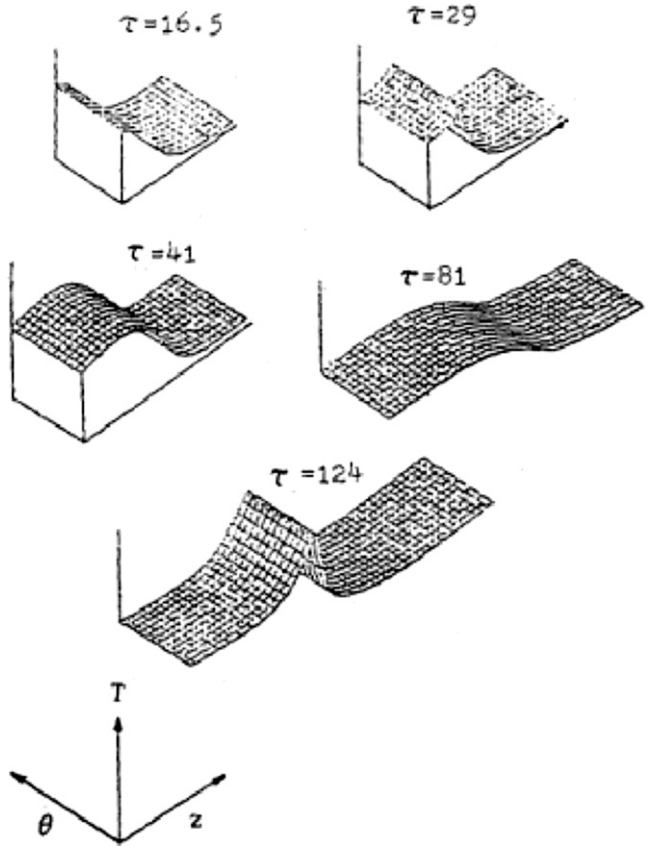

Fig. 7. Piston-like oscillatory front in two-dimensional adiabatic system. $\alpha = 0.0$, $\beta = 0.03$, $\gamma = 0.08$, $\Theta_i = -9.5$, $\Theta_o = 3.0$, $\varepsilon = 0.5$, $\delta = 0.001$, $\Delta = 0.653$.

Fig. 1. After a short transient heat-up period, the concentration and temperature profiles develop and the combustion front of constant shape occurs and moves with constant velocity. The imposed perturbation for such parameters disappears with time. The reaction front is stable locally and globally. In addition only one reaction front can exist. According to the Shkadinskii's stability analysis for an adiabatic system and a first-order reaction [2], the numerically calculated neutral stability line is given by $\Delta = 9.1\gamma - 2.5\beta$. If $\Delta \geq 1$, the stable combustion takes place. But if $\Delta < 1$, then the combustion proceeds in the unstable regime. The calculated value of $\Delta = 1.57$ for the combustion system shown in Fig. 1, may predict the existence of stable combustion front

For lower values of the parameters γ and β, the reaction front starts to oscillate and the velocity of the front depends on the time, see Figs. 2–6. For lower values of parameters γ and β comparing with those in Fig. 1, constant pattern profile front changes to simple oscillatory front as shown in Fig. 2. With further lower values of parameters γ and Θ_i, multipeak oscillations with steep flat profiles may exist in the adiabatic system as depicted in Fig. 3. For the adiabatic system with infinite activation energy, complex oscillatory front may develop and propagate downstream as shown in Fig. 4. The oscillating regimes are observed both for the adiabatic and non-adiabatic combustion systems, see Figs. 2–4. The oscillations have periodic character for the adiabatic and weakly non-adiabatic systems. Oscillations occur because the heat generated by the reaction cannot be transferred from the surface fast enough. Kim and Hlavacek [10] indicated that in the diffusion-reaction exothermic systems period-doubling bifurcation may occur which ultimately leads to chaotic behavior. The temperature can overshoot the adiabatic reaction temperature and solid reactants are completely converted. Then the temperature drops below the adiabatic reaction temperature and the fresh unreacted

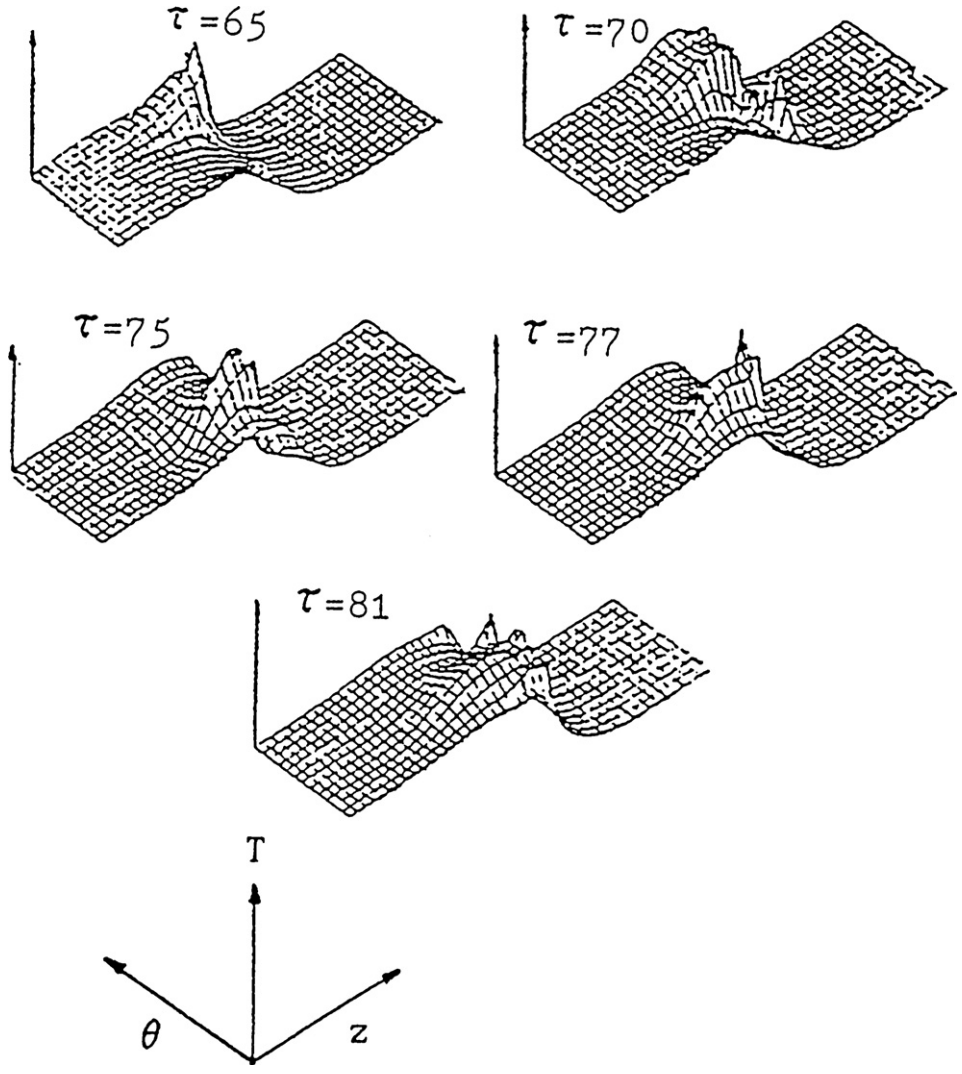

Fig. 8. Fingering waves in two-dimensional adiabatic system. $\alpha = 0.0$, $\beta = 0.03$, $\gamma = 0.08$, $\Theta_i = -9.5$, $\Theta_o = 3.0$, $\varepsilon = 0.5$, $\delta = 0.001$, Δ=0.653.

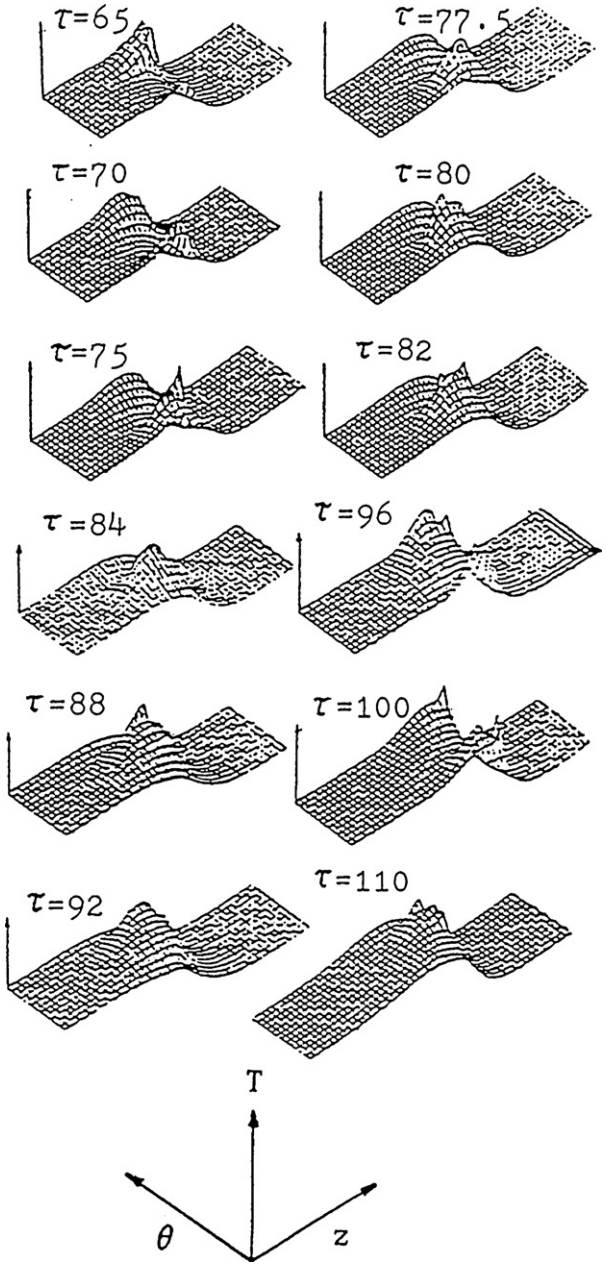

Fig. 9. Rotating waves in two-dimensional adiabatic system. $\alpha = 0.0$, $\beta = 0.03$, $\gamma = 0.08$, $\Theta_i = -9.5$, $\Theta_o = 3.0$, $\varepsilon = 0.5$, $\delta = 0.001$, $\Delta = 0.653$.

solid is slowly preheated. After the temperature reaches the critical value, the combustion reaction takes place and the temperature of reaction front again exceeds the adiabatic temperature.

The rise of surface temperature results in a very high reaction rate. If available reactant is consumed extinction occurs, see Fig. 6. During the period of a slow reaction, heat is conducted to the region with low conversion until the increasing heat generation will start the whole cycle again. The rise of surface temperature is distinctly higher for a non-adiabatic case because the reaction zone is very thin and concentration gradients are steeper than in the adiabatic case. The transient

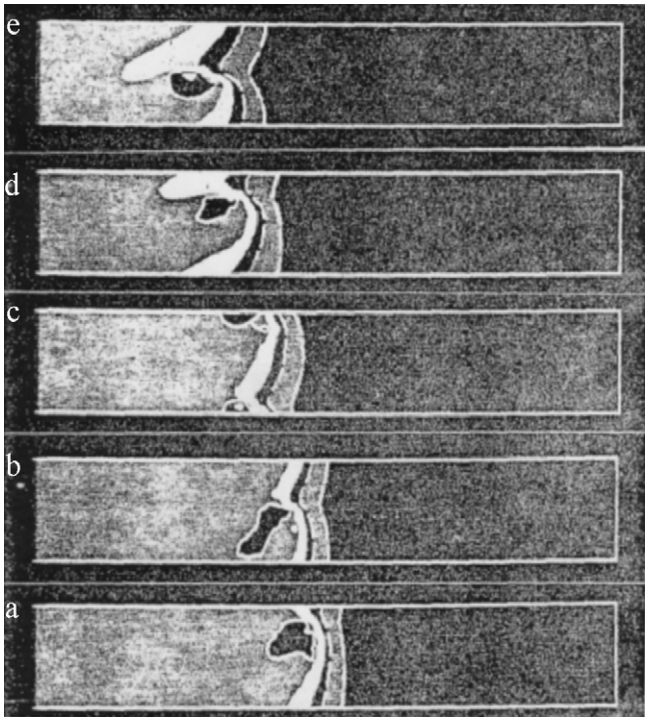

Fig. 10. Fingering waves in the tangential direction of adiabatic system. $\alpha = 0.0$, $\beta = 0.03$, $\gamma = 0.08$, $\Theta_i = -9.5$, $\Theta_o = 3.0$, $\varepsilon = 0.5$, $\delta = 0.001$, $\Delta = 0.653$.

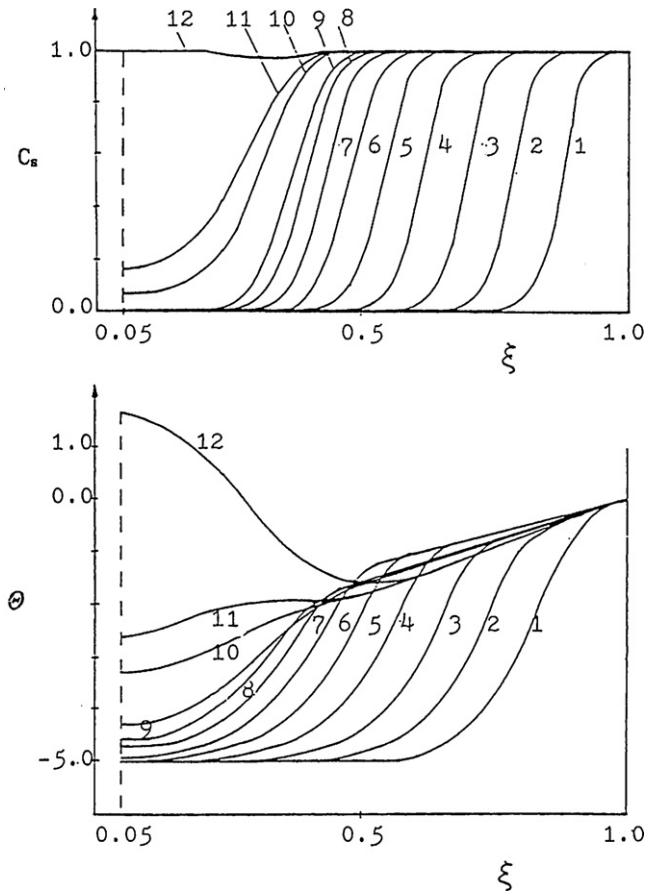

Fig. 11. Travelling waves in the radial direction for the annulus materials with the outside ignition. $\alpha = 0.0$, $\beta = 0.1$, $\gamma = 0.2$, $\Theta_i = -5.0$, $\Theta_o = 0.0$, $\varepsilon = 0.5$, $\delta = 0.00001$, $\Delta = 1.57$.

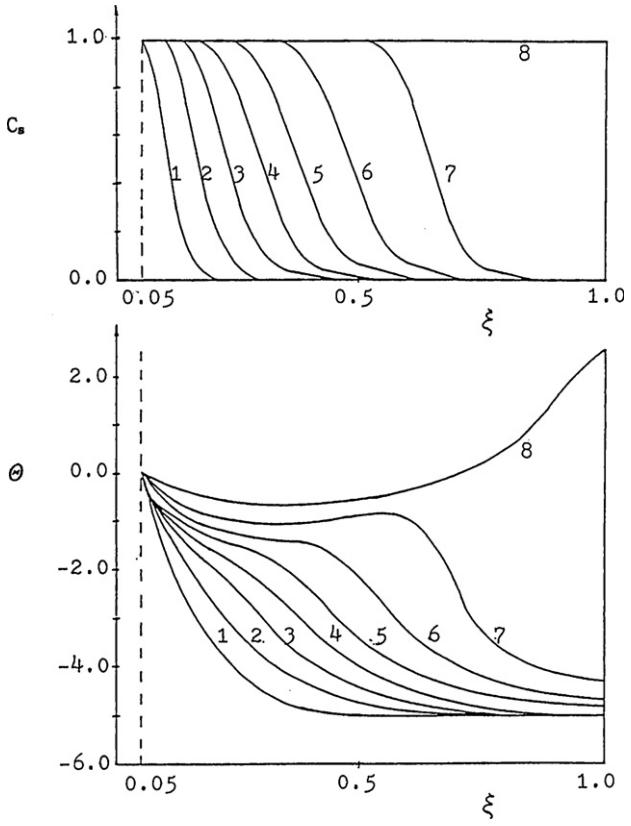

Fig. 12. Travelling waves in the radial direction for the annulus materials with the inside ignition. $\alpha = 0.0$, $\beta = 0.1$, $\gamma = 0.2$, $\Theta_i = -5.0$, $\Theta_o = 0.0$, $\varepsilon = 0.5$, $\delta = 0.00001$, $\Delta = 1.57$.

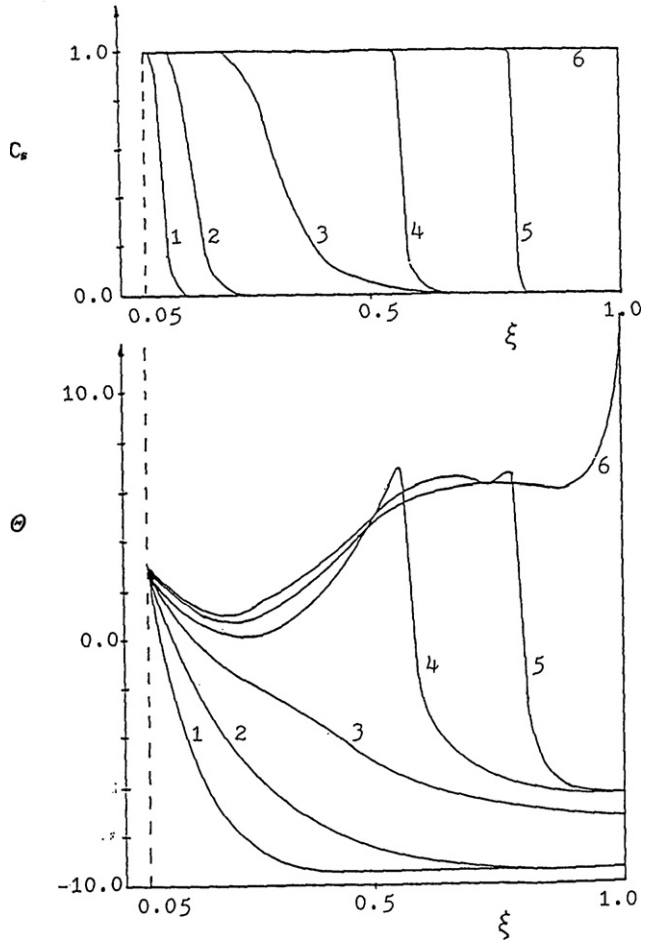

Fig. 13. Travelling waves in the radial direction for the smaller annulus materials with the inside ignition. $\alpha = 0.0$, $\beta = 0.03$, $\gamma = 0.08$, $\Theta_i = -9.5$, $\Theta_o = 3.0$, $\varepsilon = 0.5$, $\delta = 0.00001$, $\Delta = 0.653$.

temperature may rise by several hundred degrees above the adiabatic reaction temperature. Such effect can lead to the local melting of the material and finally to the nonuniform product. Extinction occurs for higher values of the heat loss parameter α as shown in Fig. 6. In such a case the material is not completely converted.

In Fig. 7, oscillating piston wave is presented. The reaction front propagates with oscillating velocity and no angular gradients. If a strong perturbation takes place in the system, the two-dimensional instability of surface combustion occurs. The type of resulting reaction fronts depends on the perturbation imposed. For a symmetrical perturbation a front results which is symmetrical with respect to this perturbation. On the other hand, for an asymmetrical perturbation an asymmetrical fingering wave occurs as depicted in Fig. 8. For a special type of perturbation a rotating wave can be triggered as shown in Fig. 9. The direction of the wave is more or less perpendicular to the axial direction. Fig. 10 clearly shows the fingering waves developing on the cylindrical sample. Merzhanov and Borovinskaya [3] experimentally observed rotating waves for the combustion of hafnium and zirconium under the environment of gaseous nitrogen. These types of waves are more stable than the piston wave because the piston wave may result in extinction of the combustion. Evidently, for strongly nonlinear situation multiple propagating fronts may exist. For identical parameter values and initial and boundary conditions, we have calculated piston, fingering, rotating, and erratic waves.

Figs. 11 and 12 represent the combustion process for the same parameters as shown in Fig. 1 but with ignition at different places. If the sample is ignited inside, the velocity of propagating profile increases with time and the temperature overshoots the adiabatic reaction temperature. If the process is ignited from the outside, the velocity of the front again is not constant but decreases with time. For larger diameter of the system the constant pattern profiles were observed in the region far enough from the center. For relatively small diameter of the sample, the temperature increases very slowly for inside ignition, see Fig. 13. If the reaction zone moves from outside to inside, the temperature after ignition increases very fast overshooting the adiabatic temperature as shown in Fig. 14. In Figs. 11–14 the profiles proceed with the time in the order of the curve number. After several oscillations, the reaction rate decreases and the region with very slow reaction is established.

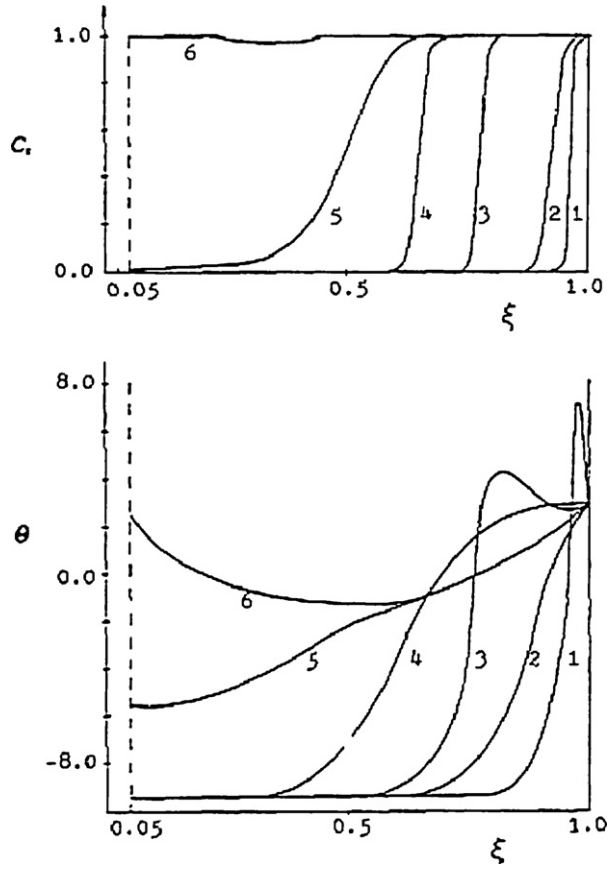

Fig. 14. Travelling waves in the radial direction for the smaller annulus materials with the outside ignition. $\alpha = 0.0$, $\beta = 0.03$, $\gamma = 0.08$, $\Theta_i = -9.5$, $\Theta_o = 3.0$, $\varepsilon = 0.5$, $\delta = 0.00001$, $\Delta = 0.653$.

4. Conclusions

The dynamic behavior of the gasless combustion on the non-adiabatic cylindrical sample was numerically investigated in the two dimensional domain. Travelling wave with constant pattern profiles are observed for adiabatic combustion systems. For lower values of parameters γ and β, the reaction front starts to oscillate and the velocity of the front depends on the time. Simple and multi-peak oscillatory fronts are detected for adiabatic and non-adiabatic combustion systems. Extinction occurs for the weakly non-adiabatic combustion system. The temperature can overshoot the adiabatic reaction temperature and the solid reactants are completely converted. For two-dimensional systems, oscillating piston wave, fingering wave, and rotating wave are developed depending on the perturbation imposed to the system.

Acknowledgements

This work was supported by the Konkuk University under Grant 2007-A019-0119.

References

[1] E.I. Maksimov, A.G. Merzhanov, V.M. Shkiro, Gasless compositions as a simple model for the combustion of nonvolatile condensed systems, Comb. Expl. Shock Waves 1 (1965) 15–18.
[2] K.G. Shkadinskii, B.I. Khaikin, A.G. Merzhanov, Propagation of a pulsating exothermic reaction front in the condensed phase, Comb. Expl. Shock Waves 7 (1971) 15–22.
[3] A.G. Merzhanov, I.P. Borovinskaya, A new class of combustion processes, Combust. Sci. Tech. 10 (1975) 195–201.
[4] P. Dimitriou, J.A. Puszynski, V. Hlavacek, On the dynamics of equations describing gasless combustion in condensed systems, Combust. Sci. Tech. 68 (1989) 101.
[5] T.P. Ivleva, A.G. Merzhanov, Three-dimensional modeling of solid-flame chaos, Dokl. Phys. Chem. 381 (2001) 259–262.
[6] T.P. Ivleva, A.G. Merzhanov, Mathematical simulation of three-dimensional spin regimes of gasless combustion, Comb. Expl. Shock Waves 38 (2002) 41–48.
[7] T.P. Ivleva, A.G. Merzhanov, Modeling of three-dimensional nonadiabatic modes of unstable solid-flame combustion, Dokl. Phys. Chem. 386 (2002) 218–221.
[8] T.P. Ivleva, A.G. Merzhanov, Concepts of solid-flame propagation modes, Dokl. Phys. Chem. 391 (2003) 171–173.
[9] C. H. Park, M.S. Thesis, State University of New York at Buffalo (1983).
[10] S.H. Kim, V. Hlavacek, On the dynamics of parabolic equation describing diffusion, convection, and chemical reaction, Physica D 10 (1984) 413.